Clinical Biomechanics 120 (2024) 106336

Contents lists available at ScienceDirect

Clinical Biomechanics

journal homepage: www.elsevier.com/locate/clinbiomech

# Biomechanical validation of a tibial critical-size defect model in minipigs

Marx Ribeiro [a,b], Vera Cora Grotheer [c,*], Luis Fernando Nicolini [d], David Latz [c], Miguel Pishnamaz [a], Johannes Greven [e], Roman Taday [c], Niklas Markus Wergen [c], Frank Hildebrand [a], Joachim Windolf [c], Pascal Jungbluth [c]

[a] Department of Orthopedics, Trauma and Reconstructive Surgery University Hospital RWTH Aachen, Pauwelstr. 30, 52074 Aachen, Germany
[b] Department of Trauma and Reconstructive Surgery University Hospital Halle, Ernst-Grube-Straße 40, 06120 Halle (Saale), Germany
[c] Department of Orthopedics and Trauma Surgery, Medical Faculty and University Hospital Düsseldorf, Heinrich Heine University, Moorenstr. 5, 40225 Düsseldorf, Germany
[d] Department of Mechanical Engineering, Federal University of Santa Maria UFSM, Av. Roraima n° 1000 Cidade Universitária Bairro – Camobi, 97105 – 900 Santa Maria, Brazil
[e] Department of Thorax Surgery, University Hospital RWTH Aachen, Pauwelstr. 30, 52074 Aachen, Germany

ARTICLE INFO

*Keywords:*
Fracture
Critical-size bone defect
Cyclic testing
Biomechanics
Minipigs

ABSTRACT

*Background:* Autologous cancellous bone grafting still represents the gold standard for the therapy of non-healing bone defects. However, donor site morbidity and the restricted availability of autologous bone grafts have initiated scientists to look for promising alternatives to heal even large defects. The present study aimed to evaluate the biomechanical potential and failure properties of a previously developed metaphyseal critical-size defect model of the proximal tibia in minipigs for future comparisons of bone substitute materials.
*Methods:* Fresh-frozen minipig tibiae were divided into two groups, with half undergoing the creation of critical-size defects. Specimens were subjected to biomechanical fatigue tests and load-to-failure tests. CT scans post-test verified bone damage. Statistical analysis compared the properties of defected and intact specimens.
*Findings:* In this model, it was demonstrated that under uniaxial cyclic compression within the loading axis, the intact tibiae specimens (8708 ± 202 N) provided a significant ($p = 0.014$) higher compressive force to failure than the tibiae with the defect (6566 ± 1653 N).
*Interpretation:* Thus, the used minipig model is suitable for comparing bone substitute materials regarding their biomechanical forces and bone regeneration capacity.

## 1. Introduction

The treatment of critical-size bone defects as a result of trauma, tumors, or pseudarthrosis is still a challenging clinical problem leading to long hospitalization and repetitive surgical interventions. In particular, bone defects of critical-size do not heal spontaneously and require special therapy. More than two million bone grafts are used per year to treat these non-healing defects (Giannoudis et al., 2005). In addition to surgical, economical, and scientific challenges, non-healing defects represent relevant socio-economic problems with serious consequences for affected patients (DeCoster et al., 2004). Delayed union or nonunion occurs in approximately 10 % of all fractures. In patients with risk factors such as diabetes mellitus or nicotine abuse, this risk increases up to 30 % (Zimmermann et al., 2006). Currently, autologous bone grafting still represents the gold standard, because of its optimal osteogenic, osteoinductive, and osteoconductive features (Fellah et al., 2008). However, besides the challenge of donor site morbidity, the restricted availability of autologous cancellous bone represents a limiting factor of its therapeutic usability (Arrington et al., 1996). Consequently, various *in vitro* and *in vivo* studies have been performed to investigate the regenerative properties of scaffolds in combination with multipotent mesenchymal stromal cells (MSCs) and/or growth factors. In this

* Corresponding author at: Department of Orthopedics and Trauma Surgery, Medical Faculty and University Hospital Düsseldorf, Heinrich Heine University Düsseldorf, Moorenstraße 5, 40225 Düsseldorf, Germany.

*E-mail addresses:* marx.ribeiro@rwth-aachen.de (M. Ribeiro), vera.grotheer@med.uni-duesseldorf.de (V.C. Grotheer), nicolini.luis@ufsm.br (L.F. Nicolini), David.Latz@med.uni-duesseldorf.de (D. Latz), mpishnamaz@ukaachen.de (M. Pishnamaz), jgreven@ukaachen.de (J. Greven), Roman.Taday@med.uni-duesseldorf.de (R. Taday), niklasmarkus.wergen@med.uni-duesseldorf.de (N.M. Wergen), fhildebrand@ukaachen.de (F. Hildebrand), Joachim.Windolf@med.uni-duesseldorf.de (J. Windolf), Pascal.Jungbluth@med.uni-duesseldorf.de (P. Jungbluth).

https://doi.org/10.1016/j.clinbiomech.2024.106336
Received 23 March 2024; Accepted 4 September 2024
Available online 7 September 2024

context, our research group has developed a large animal model in minipigs for non healing critical-size bone defects to compare and to analyze cell therapeutics for bone regeneration (Jungbluth et al., 2010). The pig exhibits nearly the same osseous-reparative capacities as humans (Schlegel et al., 2003). Therefore, its long tubular bone structure represents an ideal large animal for evaluating regenerative capacity of scaffolds, cells, and growth factors (Furst et al., 2003). Using this specific animal model, promising histomorphometrical and radiological results in the early phase of bone healing could be achieved using such as human-induced mesenchymal stromal cells (iMSCs) and autologous bone marrow concentrate (BMC) in combination with calcium phosphate granules (CPG) (Jungbluth et al., 2019; Hakimi et al., 2014). However, biomechanical studies of bone healing in critical-size defects in weight-bearing limbs in large animal models are still lacking. The present study aims to evaluate the biomechanical usability for testing the stability of bone graft substitutes in a critical-size defect model of the minipig. As previously described, no bone healing is expected with the standardized metaphyseal critical-size defect used in this study without any treatment (Hakimi et al., 2014; Jungbluth et al., 2019). For future preclinical comparison of the stability of osseous consolidation after the transplantation of bone substitute materials in a minipig model setting it is crucial to investigate the biomechanical properties of our critical-size defect (Hakimi et al., 2014).

## 2. Methods

### 2.1. Specimen and preparation

The biomechanical tests were performed on fresh-frozen minipig tibiae that had no previous defect. Animal specimens represent a suitable alternative to human bones because of their low variance in material properties (Wancket, 2015), low cost, and availability. For better comparability, the minipigs were from the same breed, had similar age and weight, and were kept under the same in-housing conditions (daily light, food, and temperature). All experiments were carried out with specimens registered at the North Rhine-Westphalia State Agency for Nature, Environment, and Consumer Protection. Ethical approval was given for all involved animals covering the Animal Welfare Act of North Rhine-Westphalia, Germany. The tibiae specimens were stored in double sealed bags in a freezer at −20 °C, thawed at 4 °C for 24 h (Robb et al., 2005), and dissected at the extremities to have a specimen length of 250 mm. Subsequently, the specimen was aligned with the knee in the most extended position. The joint and both extremities of the specimen were considered as references for alignment. Afterward, the longitudinal axis of each tibia was kept parallel to the loading axis. The proximal and distal ends were embedded in resin (Technovit® 4004, Heraeus Kulzer GmbH, Germany) using a custom-made rail system. These steps were achieved using a dual crossline laser. For 4 out of 8 specimens, a standardized monocortical critical-size defect was created by drilling a cylindrical defect of 11 mm diameter and 25 mm depth in the right proximal tibia 10 mm distal to the joint line and 12 mm anterior to the most posterior aspect of the tibia using a cannulated reamer (Aesculap AG & Co. KG, Tuttlingen, Germany), (Fig. 1 A - D) by an experienced surgeon as it was described before in our previous work (Hakimi et al., 2014; Jungbluth et al., 2010; Jungbluth et al., 2019).

### 2.2. Testing protocols

The specimens were mounted disarticulated without a femoral component in a custom-made machine (Dyna-mess Prüfsysteme GmbH, Stolberg, Germany) as shown in Fig. 2. Fatigue tests were performed using a physiological uniaxial loading protocol similar to the one performed by Weninger et al. (2009) and Tschegg et al. (2008). This protocol consists of a sinusoidal cyclic load with an average amplitude of 350 N representing the gravitational body weight of the minipig (35 kg). The compressive load oscillates up to a peak of 700 N to simulate varying loading and effects of the muscles present in daily activities (Fig. 3) (Bergmann et al., 2001; Giarmatzis et al., 2015; Kutzner et al., 2010). The specimen was set to undergo 40,000 loading cycles at 1 Hz exerted by the pneumatic actuator of the machine. The load was

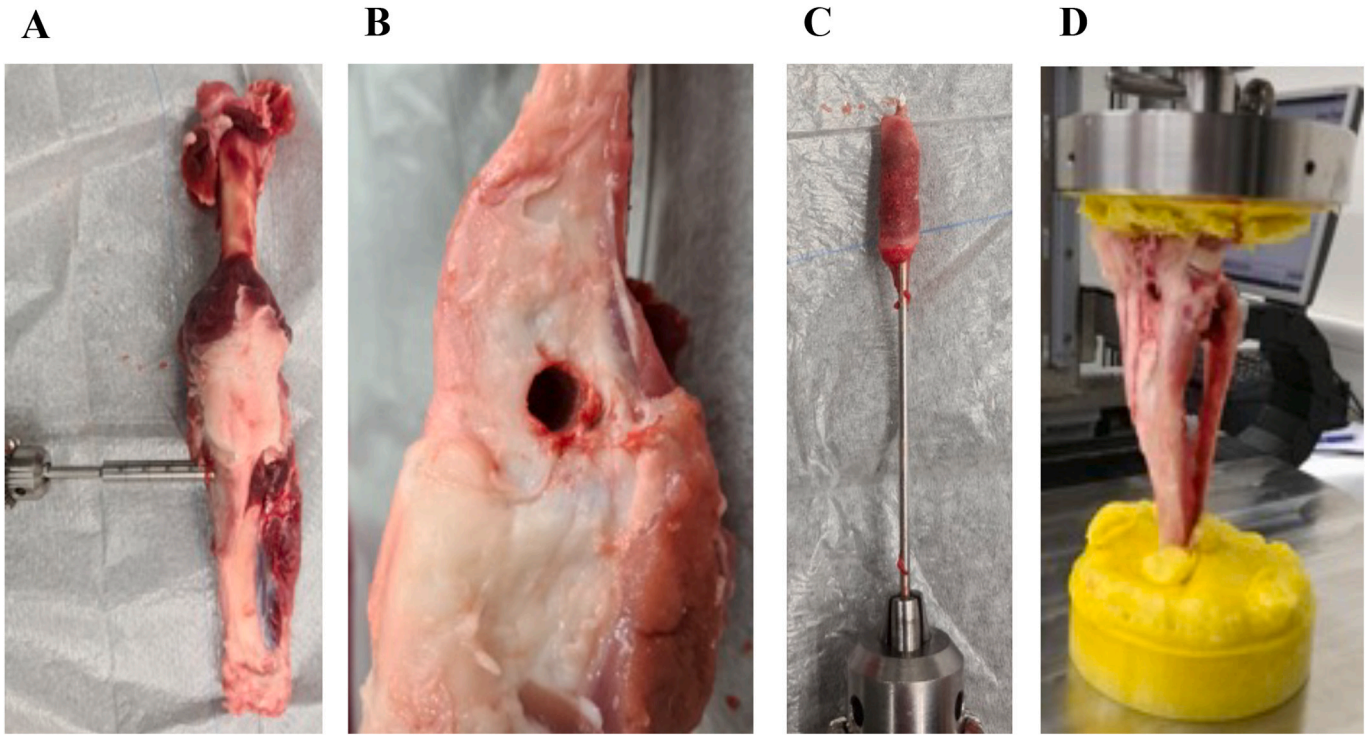


**Fig. 1.** Specimen with a standardized critical-size defect at the upper part of the tibia. (A) Positioning of the driller at the tibia (A). Close-up of the defect hole (B). Removed bone cylinder (C). Clamped tibia for fatigue test for load-to-failure analysis (D).

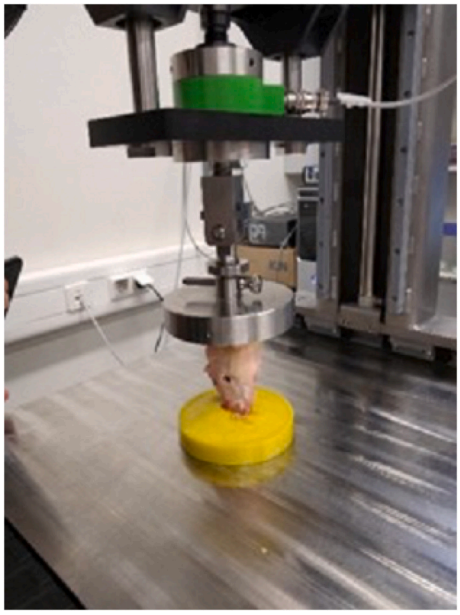

**Fig. 2.** Clamped tibia for fatigue tests at axial load machine (Dyna-Mess 2.5 kN). The compressive load was applied by a pneumatic actuator on the top of the specimen.

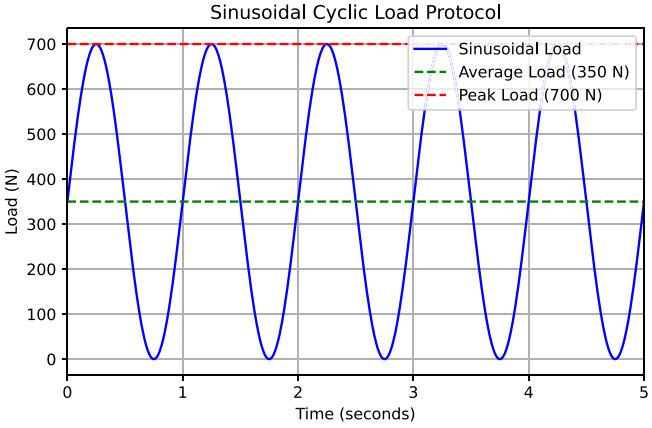


**Fig. 3.** Fatigue loading protocol used to simulate the load acting on the tibia due to the weight bearing of a minipig. A total of 40,000 cycles were performed at a frequency of 1 Hz.

recorded by a load cell at a frequency of 100 Hz. The sensor had a maximum error of 1 % relative to the target value. The diameter of the fracture defect size in the vertical direction was measured with a digital caliper before and after cyclic testing. The caliper had an accuracy of ±0.2 mm and a resolution of 0.1 mm.

Compressive load-to-failure tests were carried out using a universal machine (Zwick Roell Group, Ulm, Germany) as shown in Fig. 4. The load-to-failure protocol consisted of compression at a rate of 1 mm/s, and a reduction in load of 30 % was considered the stop criteria. Computerized tomography (CT) scans, using a 2 × 128-slice SOMATOM Definition Flash CT scanner (Siemens Healthcare AG, Zurich, Switzerland), were performed after fatigue protocol and load-to-failure tests to complement the data acquired by the machines' sensors.

### 2.3. Analysis

The CT scans were analyzed for definite signs of fracture or plastic deformation of the bone defect with the software IntelliSpace PACS

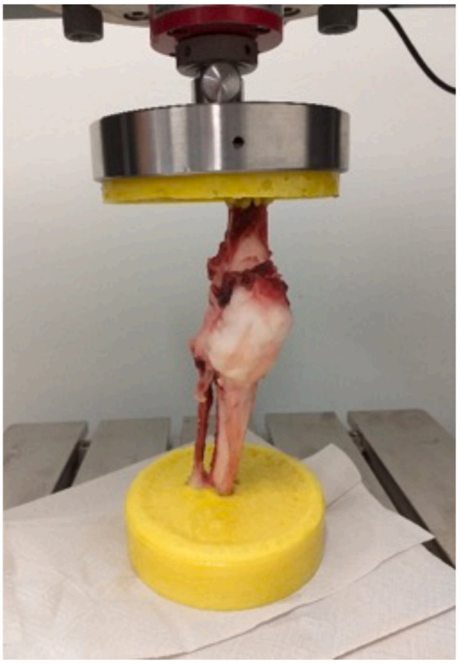

**Fig. 4.** Clamped tibia for load-to-failure test at axial load machine (Zwick-Roell 10 kN).

Enterprise (version 4.4, Phillips GmbH Market DACH Health System, Hamburg, Germany) to verify the damage to the bone after fatigue tests and after load-to-failure tests. The maximum compressive force during load-to-failure tests for the defected specimens was compared to the intact specimens. Statistical analyses were performed in Microsoft Excel (XLSTAT package) by the non-parametric Mann-Whitney *U* Test to determine statistical significance. One-tailed tests for independent samples were performed assuming a stepwise reduction in the maximum compressive force of the tibia for the intact state and defected state, respectively. The means experimental values were calculated and analyzed for statistical comparisons considering a level of significance of $p \leq 0.05$. Additionally, for the fatigue tests, the maximum displacement in compression was recorded. The comparison between defect and intact groups was performed by comparing the maximum displacement for the last cycle for the groups.

## 3. Results

### 3.1. Location of failure

After the fatigue tests the fixation of the tibiae in the axial load machine was controlled and visually confirmed to rule out loosening. The analysis of the CT scans revealed that no damage to the bone was caused by the fatigue tests, in both the defect (Fig. 5) and intact cases. No difference in the defect diameter values before and after fatigue tests was observed. However, after load-to-failure tests a fracture occurred close to the defect for all defected specimens (Fig. 6) probably explaining a stress concentration effect, and at the distal extremity of the tibia for all the intact specimens, indicating compressive overload in the structurally weakest region.

### 3.2. Fatigue tests

The results from the fatigue testing are summarized in Fig. 7, showing the mean displacement and standard deviation interval trends at maximum compression load for both intact and defect groups over 40,000 cycles relative to the initial cycle. For both groups, the displacement decreased at a higher gradient during the initial cycles of

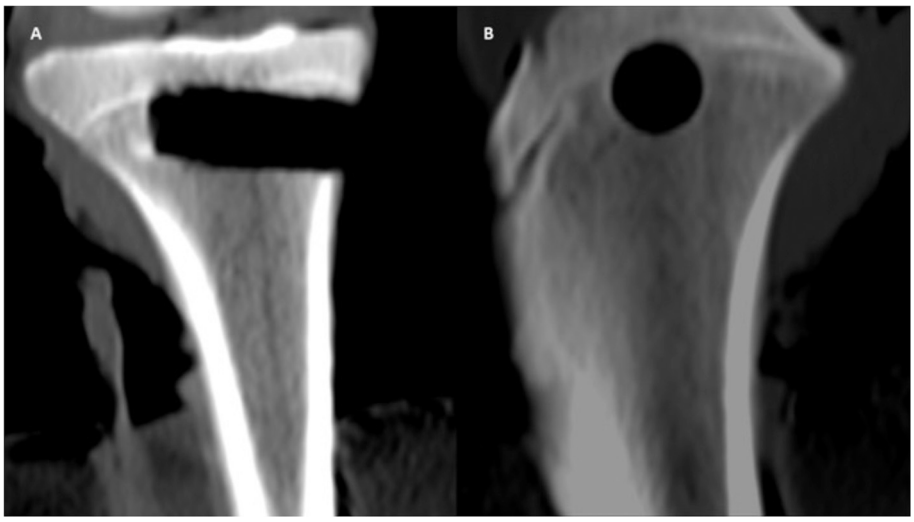


**Fig. 5.** The CT scans after the fatigue test showed an intact bone, without any sign of deformation of the critical-size defect (A: coronal plane, B: sagittal plane).

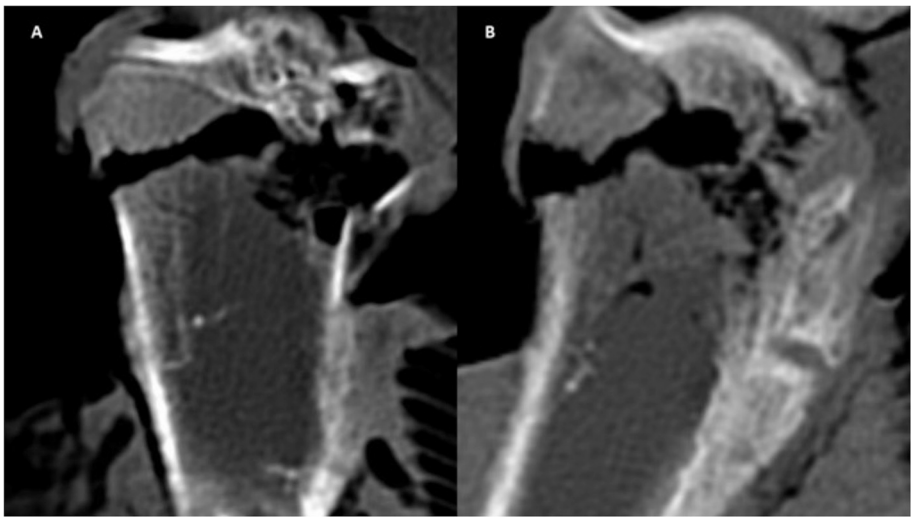


**Fig. 6.** CT scan after the load-to-failure test in a specimen with the defect. The fracture runs through the defect. (A: coronal plane, B: sagittal plane).

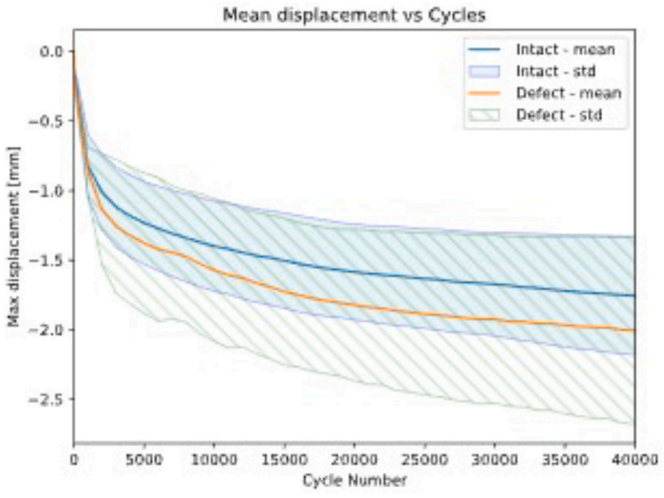


**Fig. 7.** Mean displacement [mm] of the tested group at maximum compression load over cycles. The standard deviation (std) interval is shown in the format of color area.

the test and continued to decrease throughout the observed cycle range, but at a diminishing rate. In comparison, the defect group displays a higher reduction in the mean value than the intact group. However, a higher standard deviation shown as shaded areas around the mean curves, illustrates variability with a wider dispersion in the defect group values, probably explaining a non-statistical difference between the groups. The possible statistical difference was checked with the Student's *t*-test between the groups for the final cycle providing a non-significant *p*-value ($p > 0.05$).

### 3.3. Load to failure

The values of the maximum compressive force to failure of both test groups are shown in Table 1. The maximum compressive force to failure was statistically lower in the defect specimens (6566 ± 1653 N) compared to the intact specimens (8708 ± 202 N, $p = 0.014$) as shown in Fig. 8. The defected tibia had a reduction in ultimate resistance to compressive forces of 24, 7 % on average.

## 4. Discussion

The minipig is a suitable animal model for testing failure properties

**Table 1**
Maximum compressive force obtained during load-to-failure tests.

| Specimen | Maximum compressive force (N) | |
|---|---|---|
| | Intact | Defect |
| 1 | 8837 | 6533 |
| 2 | 8885 | 7467 |
| 3 | 8437 | 8004 |
| 4 | 8672 | 4260 |
| **Average** | **8708** | **6566** |

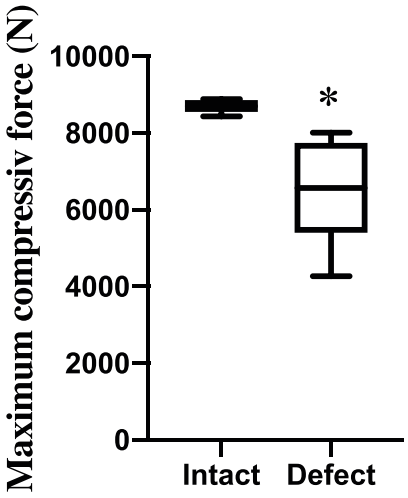


**Fig. 8.** Mean of the maximum compressive force obtained during load-to-failure tests for the intact tibia and defect tibia. Whiskers indicate min and max, line indicates the mean. The comparison between both groups was statistically significant ($p = 0.04$).

of the metaphyseal tibial bone because the bone structure of minipigs is similar to humans in terms of anatomy, morphology, remodeling rate, and comparable bone mineral density (Reichert et al., 2009). Minipigs exhibit nearly the same osseous-reparative capacities as humans, with a bone regeneration rate of 1.2 – 1.5 mm/day, and were therefore chosen as experimental species (Schlegel et al., 2003). Moreover, its' long tubular bone structure represents an ideally large animal for evaluating the regenerative capacity of scaffolds, cells, and growth factors as well as a subsequent *ex vivo* validation of osseous stability (Furst et al., 2003). The interindividual variations in the bone quality of the minipigs in this study are relatively small, because age, breed, relation, and the resulting muscle mass are comparable due to the same housing conditions. In our study, we focused on compression analysis with fatigue tests and load-to-failure test to evaluate the failure properties of the critical-size defect under compression within the loading axis. The fatigue tests were performed using a physiological and validated cyclic loading protocol similarly performed as described before by Weninger et al. (2009) and Tschegg et al. (2008). Cyclic loads were used, because they are the most direct analog to periodic stresses and strains varying in both intensity and type seen in physiological daily activities (Singhal et al., 2011; Tschegg et al., 2008). To focus on the axial stress on the metaphyseal defect, the loading was performed without the femoral component. The maximum load of 700 N simulated the forces during walking with a body weight of 87 kg to 130 kg (Neptune et al., 2001). After cyclic loads in the fatigue test, no visible or microdamage could be detected with CT scans in either intact or defected specimens. No alterations in defect diameter were observed. This effect suggests that there is sufficient fatigue strength for this critical size defect. The load-to-failure test for measuring the stiffness of a specimen is evaluated in several previous studies (Ali et al., 2006; Tschegg et al., 2008; Weninger et al., 2009; Zeng et al., 2011). The maximum compressive force to failure in our critical size defect was statistically higher in the intact specimens compared with defect specimens as shown in Fig. 8 (intact group: 8,708 ± 202 N, defect group 6,566 ± 1,653 N, $p = 0.014$). This means that peak loads have a higher probability of causing a fracture in our metaphyseal critical-size defect than in the intact ones. Repeated cyclic loading causing fatigue of the trabecular and cortical bone does not show macroscopic deformation or fracture of the critical-size defect and accordingly allows sufficient follow-up of future bone substitute analysis.

Uniaxial loading was chosen because previous studies concerning anatomical characteristics together with dynamics during gait of a quadruped's knee joint provide evidence for predominantly axial loading of the metaphyseal proximal tibia, as well as in humans (Kutzner et al., 2010; Taylor et al., 2011). Multiaxial, three-point, or four-point bending load or torsional load experiments were not applied because the study did not aim to mimic the natural forces of the knee joint. Therefore we cannot conclude that the failure mode can directly be transferred to other loading conditions. Applied load and cycles to failure showed comparably good correlations within the intact and defect group which indicates that damage occurs in a reproducible manner.

From the mechanical point of view, the location of the tibial failure for defected specimens is consistent with the effect of the stress concentration generated by the presence of a hole in the tibial structure, as shown in fracture mechanics theory, and more recently to more complex cases, by the computational use of Finite Element Method (Pilkey, 1997; Rebora and Vernassa, 2020). By the statistical analysis, we can verify a significant reduction of the maximum compression force for the defect specimens, as shown in Fig. 8. In daily activities, the body is subjected to cyclic loads that may generate microcracks of the surrounding trabecular bone structure, leading to bone fragility (Dendorfer et al., 2008; Norman et al., 1998; Wang et al., 2007). The influences of structural anisotropy on fatigue induced microcracks of the trabecular bone were not investigated in this study. The trends shown in Fig. 7 present an initial decrease in mean displacement, followed by a continuous decrease at a smaller rate, indicating a continuous adaptation to the loading conditions. This is indicative of defects acting as stress concentrators, thereby exacerbating the material's response to cyclic loading (Loundagin et al., 2021). However, the fact that the intact specimens withstood the fatigue protocol without observed damage by CT scan analysis means that possibly accumulated damage at the microscopic level did not exceed the local yield strain causing plastic deformation of the critical-size defect (Pattin et al., 1996). The observed trends align with established theories on fatigue behavior, where initial microstructural accommodation leads to a period of relative stability before eventual material degradation (Schaffler et al., 1990). This apparent stability could suggest a possible approach for scaffold or regrowth/healing studies.

A limitation of this study is that it does not analyze the local stresses and strain distributions to investigate possible relationships between loading and fracture. To the best of our knowledge, accumulated non-visible degradation in addition to geometrical brittleness caused by the hole may be responsible for the statistically significant reduction in compression strength of the group with defected specimens. Studying the failure properties of trabecular bone directed by the strain along the loading direction in this critical-size defect model supports future investigation of mechanisms of deformation in applied bone substitute materials in terms of stiffness, strength, and density (Dendorfer et al., 2009; Gibson, 1985; Niebur et al., 2002).

## 5. Conclusions

The present study aimed to validate the failure properties of our critical-size defect in the metaphyseal proximal tibia of the minipig for future comparisons of bone substitute materials in a subsequent *ex vivo* setting. It could be elucidated that in terms of cyclic uniaxial fatigue

loading and load-to-failure compression, this critical-size defect provides an appropriate animal model for future evaluation of bone graft substitutes with regard to the comparability of their failure properties.

## Funding

No funding.

## Author statement

All authors have made substantial contributions to the manuscript.

The conception and design of the study: Pascal Jungbluth, Johannes Greven, Luis Nicolini, Vera Grotheer.

Acquisition of data: Marx Ribeiro, Luis Nicolini, Niklas Wergen.

Analysis of data: Marx Ribeiro, Johannes Greven.

Drafting the article: Pascal Jungbluth, Roman Taday, David Latz, Vera Grotheer,

Revising it critically for intellectual content: Miguel Pishnamaz.

Final approval: Joachim Windolf, Frank Hildebrand.

## Manuscript statement

All related data, figures, and tables has not previously been published and the manuscript is not under consideration elsewhere.

## CRediT authorship contribution statement

**Marx Ribeiro:** Formal analysis, Data curation. **Vera Cora Grotheer:** Writing – review & editing, Writing – original draft, Conceptualization. **Luis Fernando Nicolini:** Data curation, Conceptualization. **David Latz:** Writing – original draft. **Miguel Pishnamaz:** Writing – review & editing. **Johannes Greven:** Conceptualization. **Roman Taday:** Writing – original draft. **Niklas Markus Wergen:** Data curation. **Frank Hildebrand:** Writing – review & editing. **Joachim Windolf:** Writing – review & editing. **Pascal Jungbluth:** Writing – original draft, Supervision, Project administration, Conceptualization.

## Declaration of competing interest

All authors certify that they have no affiliations with or involvement in any organization or entity with any financial interest (such as honoraria; educational grants; participation in speakers' bureaus; membership, employment, consultancies, stock ownership, or other equity interest; and expert testimony or patent-licensing arrangements), or non-financial interest (such as personal or professional relationships, affiliations, knowledge or beliefs) in the subject matter or materials discussed in this manuscript.

## References

Ali, Ahmad M., Saleh, Michael, Bolongaro, Stefano, Yang, Lang, 2006. Experimental model of tibial plateau fracture for biomechanical testing. J. Biomech. 39, 1355–1360.

Arrington, E.D., Smith, W.J., Chambers, H.G., Bucknell, A.L., Davino, N.A., 1996. Complications of iliac crest bone graft harvesting. Clin. Orthop. Relat. Res. 300–309.

Bergmann, G., Deuretzbacher, G., Heller, M., Graichen, F., Rohlmann, A., Strauss, J., Duda, G.N., 2001. Hip contact forces and gait patterns from routine activities. J. Biomech. 34, 859–871.

DeCoster, T.A., Gehlert, R.J., Mikola, E.A., Pirela-Cruz, M.A., 2004. Management of posttraumatic segmental bone defects. J. Am. Acad. Orthop. Surg. 12, 28–38.

Dendorfer, S., Maier, H.J., Taylor, D., Hammer, J., 2008. Anisotropy of the fatigue behaviour of cancellous bone. J. Biomech. 41, 636–641.

Dendorfer, S., Maier, H.J., Hammer, J., 2009. Fatigue damage in cancellous bone: an experimental approach from continuum to micro scale. J. Mech. Behav. Biomed. Mater. 2, 113–119.

Fellah, B.H., Gauthier, O., Weiss, P., Chappard, D., Layrolle, P., 2008. Osteogenicity of biphasic calcium phosphate ceramics and bone autograft in a goat model. Biomaterials 29, 1177–1188.

Furst, G., Gruber, R., Tangl, S., Zechner, W., Haas, R., Mailath, G., Sanroman, F., Watzek, G., 2003. Sinus grafting with autogenous platelet-rich plasma and bovine hydroxyapatite. A histomorphometric study in minipigs. Clin. Oral Implants Res. 14, 500–508.

Giannoudis, P.V., Dinopoulos, H., Tsiridis, E., 2005. Bone substitutes: an update. Injury 36 (Suppl. 3), S20–S27.

Giarmatzis, G., Jonkers, I., Wesseling, M., Van Rossom, S., Verschueren, S., 2015. Loading of hip measured by hip contact forces at different speeds of walking and running. J. Bone Miner. Res. 30, 1431–1440.

Gibson, L.J., 1985. The mechanical behaviour of cancellous bone. J. Biomech. 18, 317–328.

Hakimi, M., Grassmann, J.P., Betsch, M., Schneppendahl, J., Gehrmann, S., Hakimi, A.R., Kropil, P., Sager, M., Herten, M., Wild, M., Windolf, J., Jungbluth, P., 2014. The composite of bone marrow concentrate and PRP as an alternative to autologous bone grafting. PLoS One 9, e100143.

Jungbluth, P., Wild, M., Grassmann, J.P., Ar, E., Sager, M., Herten, M., Jager, M., Becker, J., Windolf, J., Hakimi, M., 2010. Platelet-rich plasma on calcium phosphate granules promotes metaphyseal bone healing in mini-pigs. J. Orthop. Res. 28, 1448–1455.

Jungbluth, P., Spitzhorn, L.S., Grassmann, J., Tanner, S., Latz, D., Rahman, M.S., Bohndorf, M., Wruck, W., Sager, M., Grotheer, V., Kröpil, P., Hakimi, M., Windolf, J., Schneppendahl, J., Adjaye, J., 2019. Human iPSC-derived iMSCs improve bone regeneration in mini-pigs. Bone Res. 7, 32.

Kutzner, I., Heinlein, B., Graichen, F., Bender, A., Rohlmann, A., Halder, A., Beier, A., Bergmann, G., 2010. Loading of the knee joint during activities of daily living measured in vivo in five subjects. J. Biomech. 43, 2164–2173.

Loundagin, L.L., Pohl, A.J., Edwards, W.B., 2021. Stressed volume estimated by finite element analysis predicts the fatigue life of human cortical bone: the role of vascular canals as stress concentrators. Bone 143, 115647.

Neptune, R.R., Kautz, S.A., Zajac, F.E., 2001. Contributions of the individual ankle plantar flexors to support, forward progression and swing initiation during walking. J. Biomech. 34, 1387–1398.

Niebur, G.L., Feldstein, M.J., Keaveny, T.M., 2002. Biaxial failure behavior of bovine tibial trabecular bone. J. Biomech. Eng. 124, 699–705.

Norman, T.L., Yeni, Y.N., Brown, C.U., Wang, Z., 1998. Influence of microdamage on fracture toughness of the human femur and tibia. Bone 23, 303–306.

Pattin, C.A., Caler, W.E., Carter, D.R., 1996. Cyclic mechanical property degradation during fatigue loading of cortical bone. J. Biomech. 29, 69–79.

Pilkey, Walter D., 1997. Peterson's Stress Contraction Factors, 2nd edition (New York).

Rebora, Alessandro U., Vernassa, Gianluca, 2020. Transverse circular holes in cylindrical tubes loaded in traction and in flexion: a new analytical approximation of the stress concentration factor. Materials 13, 1331.

Reichert, J.C., Saifzadeh, S., Wullschleger, M.E., Epari, D.R., Schütz, M.A., Duda, G.N., Schell, H., van Griensven, M., Redl, H., Hutmacher, D.W., 2009. The challenge of establishing preclinical models for segmental bone defect research. Biomaterials 30, 2149–2163.

Robb, J.L., Cook, J.L., Carson, W., 2005. In vitro evaluation of screws and suture anchors in metaphyseal bone of the canine tibia. Vet. Surg. 34, 499–508.

Schaffler, M.B., Radin, E.L., Burr, D.B., 1990. Long-term fatigue behavior of compact bone at low strain magnitude and rate. Bone 11, 321–326.

Schlegel, K.A., Kloss, F.R., Schultze-Mosgau, S., Neukam, F.W., Wiltfang, J., 2003. Osseous defect regeneration using autogenous bone alone or combined with biogran or Algipore with and without added thrombocytes. A microradiologic evaluation. Mund Kiefer Gesichtschir. 7, 112–118.

Singhal, A., Aimer, J.D., Haeffner, D.R., Dunand, D.C., 2011. High-energy X-ray diffraction measurement of bone deformation during fatigue. In: Conference Proceedings of the Society for Experimental Mechanics Series, pp. 395–398.

Taylor, W.R., Poepplau, B.M., König, C., Ehrig, R.M., Zachow, S., Duda, G.N., Heller, M. O., 2011. The medial-lateral force distribution in the ovine stifle joint during walking. J. Orthop. Res. 29, 567–571.

Tschegg, Elmar K., Herndler, Stefan, Weninger, Patrick, Jamek, Michael, Stanzl-Tschegg, Stefanie, Redl, Heinz, 2008. Stiffness analysis of tibia-implant system under cyclic loading. Mater. Sci. Eng. C 28, 1203–1208.

Wancket, L.M., 2015. Animal models for evaluation of bone implants and devices: comparative bone structure and common model uses. Vet. Pathol. 52, 842–850.

Wang, X., Masse, D.B., Leng, H., Hess, K.P., Ross, R.D., Roeder, R.K., Niebur, G.L., 2007. Detection of trabecular bone microdamage by micro-computed tomography. J. Biomech. 40, 3397–3403.

Weninger, P., Schueller, M., Jamek, M., Stanzl-Tschegg, S., Redl, H., Tschegg, E.K., 2009. Factors influencing interlocking screw failure in unreamed small diameter nails–a biomechanical study using a distal tibia fracture model. Clin. Biomech. (Bristol, Avon) 24, 379–384.

Zeng, Z.M., Luo, C.F., Putnis, S., Zeng, B.F., 2011. Biomechanical analysis of posteromedial tibial plateau split fracture fixation. Knee 18, 51–54.

Zimmermann, G., Moghaddam, A., Wagner, C., Vock, B., Wentzensen, A., 2006. Clinical experience with bone morphogenetic protein 7 (BMP 7) in nonunions of long bones. Unfallchirurg 109, 528–537.